

EXAMINATION OF PAINTING TECHNIQUE AND MATERIALS OF LIU KANG'S SEAFOOD AND HIDDEN SELF-PORTRAIT

Damian LIZUN^{1,*}, Paweł SZROEDER², Teresa KURKIEWICZ³, Bogusław SZCZUPAK⁴

¹ Heritage Conservation Centre, National Heritage Board, 32 Jurong Port Rd, 619104, Singapore

² Institute of Physics, Kazimierz Wielki University, Al. Powstańców Wielkopolskich 2, 85-090, Bydgoszcz, Poland

³ Department of Painting Technology and Techniques, Institute for Conservation, Restoration and Study of Cultural Heritage, Nicolaus Copernicus University, ul. Sienkiewicza 30/32, 87-100, Toruń, Poland

⁴ Department of Telecommunications and Teleinformatics, Wrocław University of Science and Technology, Wybrzeże Stanisława Wyspiańskiego 27, 50-370, Wrocław, Poland

Abstract

*This paper is a part of an ongoing research that aims to present the painted oeuvre of pioneering Singapore artist Liu Kang (1911 – 2004) through the lens of conservation science instruments. The study concentrates on the painting *Seafood* from the National Gallery Singapore collection. The painting was created in 1932 and represents Liu Kang's early artistic period, "Paris". The painting was studied using complementary examination techniques. The imaging methods, including digital microscopy, NIR, XRR and RTI, revealed a hidden painting underlying the existing composition. XRR and NIR provided strong evidence that the image underneath is a portrait of a man while RTI revealed its texture. A comparative stylistic study of the hidden portrait was conducted with two other of Liu Kang's self-portraits from the same period. The study exposed some similarities, leading to the conclusion that the hidden painting is Liu Kang's self-portrait. Results of these imaging techniques initiated a further in-depth study to characterise and compare the pigments used in the creation of *Seafood* and that of the hidden self-portrait. The pigments of these two paintings were identified by means of IRFC, SEM-EDS, FTIR, PLM and XRF. Additionally, the in-depth study increased our understanding of both pictures and contributed to the growing body knowledge about Liu Kang's "Paris" period.*

Keywords: IRFC; X-RAY; RTI; SEM-EDS; FTIR; Liu Kang; Hidden painting; Lefranc paints

Introduction

Liu Kang (1911 – 2004), on graduating from Xinhua Arts Academy in Shanghai, moved to Paris in an attempt to assimilate the artistic essence of the Western masters. According to his travel documents, which were shared by the Liu family, he arrived in France in February 1929 and stayed there until April 1932. During that time, he was drawn to Impressionist, Post-Impressionist and Fauvist masters, whose works influenced his own [1]. His career took off in 1930 and 1931 with the annual art exhibition Salon d'Automne, where he exhibited his paintings. The painting *Seafood* (1932), from the National Gallery Singapore collection, represents that period in his artistic carrier (Fig. 1).

The analysed case study is *Seafood*, an oil-on-canvas painting measuring 46 × 55cm. The painting is a straightforward still life, depicting the main subject – a red lobster on a white plate – in the centre. A green fruit placed near the lobster breaks this almost-centrist

* Corresponding author: damian_lizun@nhb.gov.sg

composition and subtly pulls some attention away from the lobster. The tilted tabletop, with the flattening and merging of planes, manifest the influence of Paul Cézanne's still lifes, while the implementation of strong, dark contour lines to delineate objects is reminiscent of Paul Gauguin's artistic style. Although it is a static composition, it exudes great spontaneity, in the paint application, and power, which is expressed in the vivid red colour of the lobster and enhanced by its strong contrast to the white plate. The palette is limited to five colours – red, white, green, brown and black – and all have subtle tonal nuances across the painting. The painting is signed, with a Chinese character Kang (抗), and dated in the Western style (1932); that is, horizontally in the bottom-left corner.



Fig. 1. Liu Kang, *Seafood*, 1932, oil on canvas, 46 × 55cm. Gift of the artist's family. Collection of National Gallery Singapore. The white arrows indicate the sampling areas

Already at first glance, *Seafood* possesses some intriguing paint features that do not correlate to the final composition. Several bold, curved and dark paint strokes and patches are visible on the brown tabletop and white plate. On the one hand, these features blend with the existing elements, enriching the overall tonality and adding some spontaneity. On the other hand, some other features cause a visible disturbance, creating an impression of an uneven table surface. To obtain more information about the artist's technique and the materials he used, the painting was investigated for the first time by means of non- and micro-invasive methods. Initial close inspection revealed the existence of an underlying painting scheme. While this was an interesting discovery, further imaging methods brought to light a much more exciting finding – the portrait of a man. At that point, a comprehensive investigation was initiated to fully identify the composition details of the portrait and understand the artist's choice of materials for both paintings.

Although it is unknown what brand of colours Liu Kang used during his stay in Paris, Liu family records show that the artist had some interest in Lefranc paints as he had preserved and brought home two pages from the October 1928 Lefranc catalogue, which contains a list of oil colours (*finés*) and their prices (Fig. 2). While that may not be a compelling evidence to draw firm conclusion about the brand of colours that the artist preferred, authors of this study reviewed Lefranc catalogues from 1928 to 1934 and will make some references in relation to certain pigments.



Fig. 2. Oil colours (*fin*s) listed in a Lefranc catalogue, Paris, October 1928. Detail showing two pages of the catalogue that Liu Kang preserved and brought home. Liu Kang Family Collection. Images courtesy of Liu family

Materials and Methods

Technical photography

The technical images were acquired according to the workflow described by A. Cosentino [2-4]. A Nikon D90 DSLR modified camera with a sensitivity of between about 360 and 1100nm was used. The camera was calibrated with X-Rite ColorChecker Passport. Visible and ultraviolet fluorescence (UVF) photography at 365nm were taken with X-Nite CC1 and B+W 415 filters coupled together. For near-infrared (NIR) imaging at 1000nm Heliopan RG1000 filter was used while Andrea “U” MK II filter was used for reflected ultraviolet photography (UVR).

The illumination system for visible and NIR photography consisted of two 500W halogen lamps while two lamps equipped with eight 40W 365nm UV fluorescence tubes were used for UVF and UVR photography.

The American Institute of Conservation Photo Documentation (AIC PhD) target was used for the images’ white balance and exposure control. Further processing of the photographs including false-colour infrared imaging (IRFC) was carried out with Adobe Photoshop CC according to the standards set out by the American Institute of Conservation [5].

High-resolution Digital Microscopy

The paint layer was examined with a Keyence VHX-6000 digital microscope, using universal zoom lenses coupled with a high-speed camera. Observations were conducted with a magnification range of 20 – 50×. For analysis, a built-in Keyence software – VHX-H2M2 and VHX-H4M – was used.

Reflectance Transformation Imaging

Reflectance Transformation Imaging (RTI) and further processing of the images using Adobe Photoshop, RTIBuilder and RTIViewer software were carried out according to the workflow proposed by the Cultural Heritage Imaging [6-8].

X-ray Radiography

The painting was digitally X-ray radiographed (XRR) using a Siemens Ysio Max Digital X-ray System with a detector size 35 × 43cm and high pixel resolution (over 7 million pixels) in the detector face. The X-ray tube operated at 40kV and 0.5-2mAs. The four images were first processed with an X-ray medical imaging software, iQ-LITE, then exported to Adobe Photoshop CC for final alignment and merging.

X-ray Fluorescence

Portable X-ray fluorescence (XRF) spectroscopy analysis was performed with Thermo Scientific™ Niton™ XL3t 970 spectrometer with a GOLDD+ detector, and an Ag anode X-ray tube with a 6 – 50kV voltage and up to 200µA current. A mining mode with four elemental ranges and measurement duration of 50s each (total acquisition time of 200s) was activated to achieve better sensitivity for light elements. The spectra were collected from a 3mm diameter spot size. The instrument was supported on a tripod. The acquired spectra were collected and interpreted using Thermo Scientific™ Niton Data Transfer (NDT™) 8.4.3 software, which allowed the elemental characterisation of the analysed spots. The XRF instrument was used for the acquisition of spectra from one area where sampling was not safe.

Scanning electron microscope with energy dispersive spectroscopy

The cross-sections of the paint samples were mounted on carbon tapes and examined with a Hitachi SU5000 Field Emission Scanning Electron Microscope (FE-SEM) coupled with Bruker XFlash® 6/60 energy dispersive X-ray spectroscopy (EDS). The SEM, backscattered electron mode (BSE), was used in 60Pa vacuum, with 20kV beam acceleration, at 50–60 intensity spot and a working distance of 10mm. The distribution of chemical elements was mapped using the Bruker Esprit 2.0 processing software.

Fourier transform infrared spectroscopy

Attenuated total reflectance-Fourier transform infrared spectroscopy (ATR-FTIR) was carried out using a Bruker Hyperion 3000 FTIR microscope with a mid-band MCT detector, coupled to a Vertex 80 FTIR spectrometer. Measurements were carried out in the spectral range of 4000–600cm⁻¹, at a resolution of 4cm⁻¹, averaging 64 scans. The elaboration of spectra was done using Bruker Opus 7.5 software.

Optical Microscopy and Polarized Light Microscopy

Optical microscopy (OM) of samples was performed in visible and ultraviolet reflected light on a Leica DMRX polarized microscope with a magnification range of 40 – 200×. Polarized light microscopy (PLM) was carried out in visible transmitted light at magnifications of 100 – 400× using the methodology developed by *P. Mactaggart and A. Mactaggart* [9]. The OM and PLM images were taken with a Leica DFC295 digital camera coupled with the microscope.

Staining test

The iodine test was conducted with a fresh KI₃ solution on the cross-section of the paint layer to determine the presence of starch [10].

Samples

A total of 15 micro-samples of the paint layer were taken from the areas of existing losses. Samples for cross-section structure observation and analysis were embedded in a fast-

curing acrylic resin, ClaroCit (supplied by Struers), and fine polished. Samples for PLM were mounted with Cargille Meltmount nD = 1.662.

Results and Discussion

The surface painting: Seafood

Ground layer

The technical photography of the painting's surface followed by analyses of the cross-sections of the paint layer revealed that *Seafood* was painted on the underlying composition without the application of an intermediate ground.

Brown

The parts painted with different shades of brown are imaged yellow-green in the IRFC, suggesting the use of ferrous pigment(s) (Fig. 3).



Fig. 3. IRFC image of *Seafood*

The purple hue that is mostly visible on the tabletop has its source in an underlying green paint, which will be investigated later. Two samples, light brown (sample 4b) and dark brown (sample 13), were investigated with SEM-EDS and PLM. A strong Fe-signal from both samples, detected with SEM-EDS, can be attributed to brown iron oxide, which is confirmed with PLM (anisotropic brown particles with a high refractive index). The high content of Pb, Cr and Ca indicated the presence of chrome yellow (lead chromate), which was confirmed with PLM observation (anisotropic particles between crossed polarized filters have the shape of tiny rods with a high refractive index). Presence of Ca may relate to chalk (calcium carbonate) added commercially to chrome yellow to obtain a lighter shade or to improve the handling properties of the paint. Chalk can also appear as a by-product in the production of chrome yellow [11]. It is uncertain if a mix of iron oxide and chrome yellow from the dark brown paint (sample 13) was obtained by the artist or commercially prepared. Ochres can be commercially enhanced by a small addition of chrome yellow [12, 13], usually extended with barium white (barium sulphate), kaolin, gypsum (calcium sulphate) and calcium chromate [12]. The detection of Ca- and P-signals suggested a small admixture of bone black later confirmed with PLM (anisotropic grey and black particles).

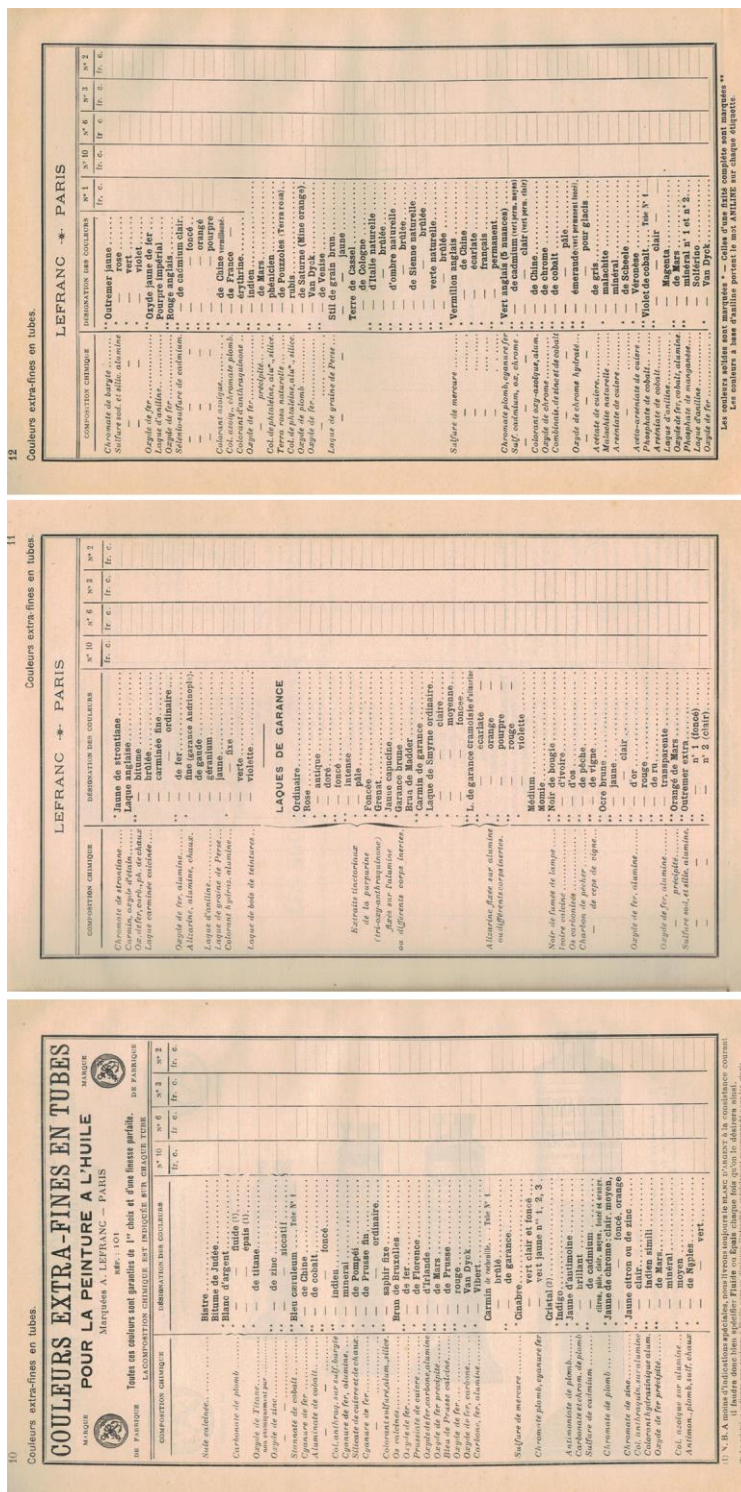


Fig. 4. Oil colours (*extra-fines*) listed in the catalogue of Lefranc, Paris 1930. Detail showing carmines, range of madder lakes, Hansa red, Hansa yellow, strontium yellow, emerald green and Scheele’s green as being available

Pinpointing the source of the other elements, such as Mg, Al, Si, P, K, Zn and As, is difficult, however they coincide naturally with iron oxides [13]. Traces of Sr found in the light brown paint (sample 4b) may indicate a common impurity of barium white [14, 15] rather than strontium yellow (strontium chromate). However, it is worth noting that strontium yellow was listed in the Lefranc catalogues of oil paints (*extra-fines*) as *chromate de strontiane* (Fig. 4), and its chemical composition was confirmed in the recent analysis of the set of Lefranc oil paints from the early 1930s [16].

Green

Light, green fruit was imaged violet in IRFC, indicating a presence of a complex paint mixture, while the dark, green background appears dark purple in the IRFC, suggesting a probable use of Cr- and/or Co-containing green pigment (Figs. 1 and 3). SEM-EDS of both samples 7 and 3 detected a similar set of elements, but with different concentrations and excluded the presence of cobalt.

Light green (Figs. 5a and b) is characterised by strong Pb-, Ba-, Cr- and S-signals, suggesting a presence of viridian (hydrated chromium oxide), chrome yellow and barium white. Viridian was observed with PLM by large particles, with a rough surface and high refractive index. Chrome yellow was observed with PLM and confirmed with FTIR by peaks at 625, 847 cm^{-1} (CrO_4^{2-} symmetric stretching), 1034, 1059, 1104, 1146 cm^{-1} [17]; however, the confirmation of the presence of barium white was hampered by overlapping signals for chrome yellow. Barium white was in common use as an extender, among others, for viridian [18] and chrome yellow [12]. The presence of chalk, which is probably an admixture to chrome yellow, was confirmed with FTIR by peaks at 872 and 1410 cm^{-1} . The concomitant presence of Cu and As elements evidenced the use of emerald green (copper acetoarsenite) and/or Scheele's green (copper arsenite). *Vert Veronese* (emerald green), *vert de Scheele* (Scheele's green) and its variant, *vert minérale*, appeared in the Lefranc catalogues of oil paints (*extra-fines*) (Fig. 4). Emerald green was confirmed with FTIR by the detection of the As-O stretch at 818 cm^{-1} and ester group stretching peak at 1569 cm^{-1} [19]. The PLM observation could not make any attribution, probably due to an insufficient quantity of the pigment in question in the sample. The SEM-EDS detection of Fe, as well as the PLM observation of very few sporadic brown and blue particles, allowed the identification of the brown iron oxide and Prussian blue (dark blue, isotropic particles with a low refractive index that appear dark greenish with a Chelsea filter). Prussian blue (hydrated iron hexacyanoferrate) is known for its very high tinting strength, achieved with at low concentration of pigment. Thus, the FTIR was able to detect a weak absorption peak at 2097 cm^{-1} , attributable to $\text{C}\equiv\text{N}$ stretching [20]. These analyses are in agreement with the IRFC imaging, as a purple representation of viridian combined with a grey blue representation of emerald green and a dark blue representation of Prussian blue can produce violet.

Dark green (Figs. 5c and d) contains a high concentration of Cr and PLM observation allowed the identification of a good deal of viridian particles in the paint sample. The detection of strong Cu- and As-signals with SEM-EDS suggests the use of Scheele's or emerald green however the PLM observation of the paint sample was inconclusive. Nevertheless, as emerald green was detected in sample 7, it is more likely that it is present in the dark green paint. Ba and S could be attributed to the barium white extender for viridian. The Fe-signal detected with SEM-EDS correlates with the dark brown particles observed on the cross-section of the paint, suggesting the presence of brown iron oxide, later confirmed with PLM. Other elements like Ca, Pb and Cr could be linked with iron oxide or Cr-containing yellow pigment(s) not identified with PLM. These findings are consistent with the IRFC imaging, as a purple colour is determined by a high content of viridian in the analysed paint.

As emerald green and viridian were detected in both, light and dark green mixtures, it is difficult to ascertain whether these two pigments were deliberately mixed by artist or emerald green was commercially adulterated with viridian [21].

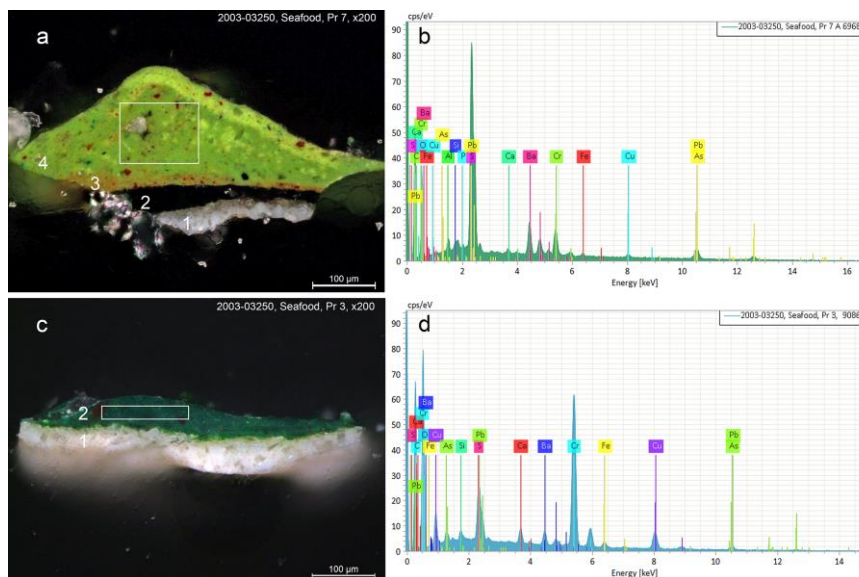


Fig. 5. Cross-sections and corresponding SEM-EDS spectra of green layers from samples 7 (a, b) and 3 (c, d).

The SEM-EDS quantitative elemental analysis shows that the intensity of the green colour in both samples is determined by the presence of chrome yellow and viridian rather than the emerald green.

The cross-section of sample 7 shows no evidence of an intermediate ground layer between the two painted compositions (layers 2 and 3)

Red

The red paint used for painting of the lobster is not uniform and is characterised by different hues of red, which gradually turns brown in the shadows and yellow in the highlights (Fig. 1). A microscopic observation of the lobster's surface and paint sample cross-section (sample 21) revealed a wet-in-wet paint application (Figs. 6 and 8a). The cross-section of the paint sample shows two layers (red and purple) without a clear division between them. The upper red consists of clusters of not properly mixed colours of dark red, red and orange. The PLM allowed the preliminary identification of the organic red pigment, due to its unique low refractive index. FTIR measurements, although very challenging due to interfering signals of the oil binder and other inorganic components, confirmed alizarin crimson by typical absorption bands at 606, 669, 1249, 1387, 1552, 1591, and 1627 cm^{-1} (Fig. 7a) [22]. Moreover, the presence of Hansa red was confirmed by absorption peaks at 753, 1256, 1297, 1345, 1448, 1467, 1502, 1560 and 1621 cm^{-1} (Fig. 7b). In addition, the PLM observation of crystalline sublimates and FTIR detection of peaks at 750, 1353 and 1518 cm^{-1} confirmed the presence of Hansa yellow (Fig. 7a). SEM-EDS, FTIR and PLM identified also lead white (lead carbonate), barium white, chrome yellow and chalk present in the paint mixture. A co-location of Cr- and Ca-signals, visible in the SEM-EDS elemental distribution maps, suggests that chalk was an admixture to chrome yellow (Fig. 6).

Although these results require further investigation, Lefranc's catalogues give some insight into the availability of natural and synthetic madder pigments. According to Lefranc's description of the chemical composition of the pigments, there were available madder lakes derived from *purpurine* (*tri-oxy-anthraquinone*) along with different pink colours containing chrome yellow, anthraquinone and azo pigments. In addition, Lefranc listed *jaune permanent moyen*, which contains Hansa yellow (*colorant azoïque sur alumine*) and *rouge de Chine vermillonné* containing Hansa red (*colorant azoïque*) (Fig. 4). Although occurrences of Hansa yellow are relatively limited in artworks prior to 1950, the recent analysis of early-20th century Lefranc lake and synthetic organic pigments provided evidence that azoic dyes, like Hansa yellow and Hansa red, were added as a component to other paints [23].

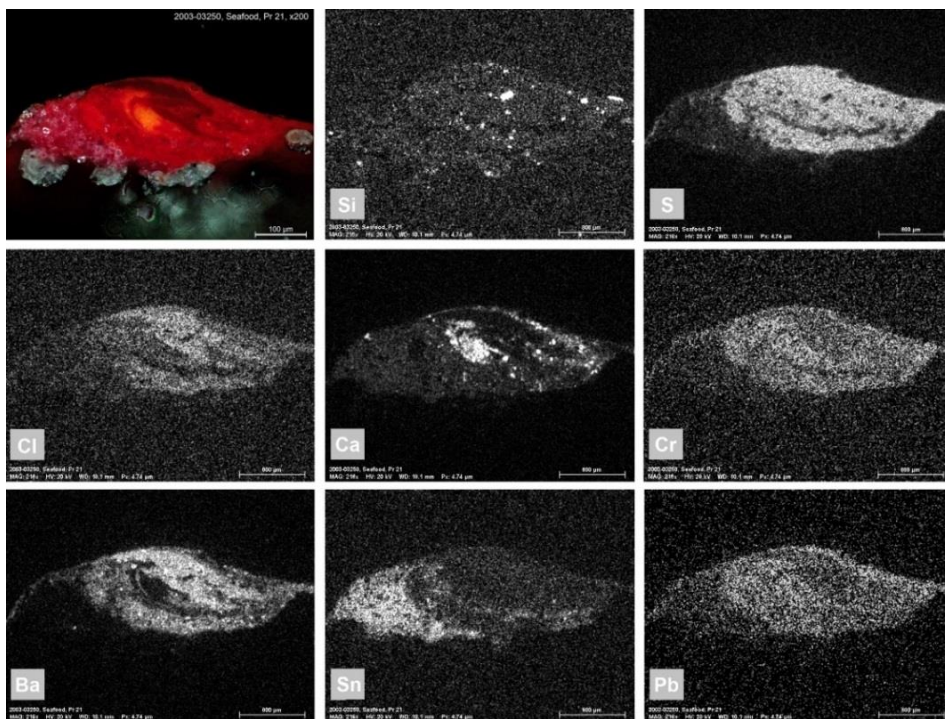


Fig. 6. Microscopy image of the cross-section of sample 21, photographed in visible light, and SEM-EDS maps showing the distribution of the detected elements. The greyscale corresponds to the intensity of the signal of each element: white equals high intensity, black means low intensity. A high concentration of Sn relates to the presence of a tin-based substrate in the paint

For the bottom purple layer, PLM allowed the detection of an organic red pigment while the FTIR analysis revealed the presence of brazilwood (absorption bands 669 , 1024 and 1562cm^{-1}) [24] and alizarin crimson (1118 and 1540cm^{-1}) [21] (Fig. 7c). In addition, starch grains were observed with PLM by round particles with a distinct extinction cross, which was visible in polarized light (Fig. 8c).

The presence of starch was positively confirmed with the iodine test and FTIR measurements showing peaks at 993 , 1074 , 1381 , 1641 , 2930 , 2965 and 3317cm^{-1} (Fig. 7c) [25]. The occurrence of starch in the bottom layer correlates with the high concentration of Sn, detected with SEM-EDS (Fig. 6), suggesting the presence of a tin-based substrate in the paint. Tin is described in the literature as a complexing ion, commonly associated with cochineal lake pigments to produce intense red hues [26, 27].

Meanwhile, starch is known as a substrate or an inert additive, used to obtain a lighter shade of the organic red pigment and improve its handling properties [27, 28]. Tin was also employed as a substrate for the brazilwood pigment; such a combination was encountered in Vincent van Gogh's paintings [29]. Brazilwood, as a cheap type of organic red, was often added to other types of lakes to reduce the cost of manufacturing [29]. The SEM-EDS detection of other elements in the purple layer, like Pb, Ba, Ca, Al and S, is difficult to interpret due to their weak signal; however, it is known that lead white, barium white, chalk and kaolin may occasionally accompany the organic red pigment [25, 27]. Lefranc listed *carmin de cochenille* and *laque anglaise* containing *carmin* and *oxyde d'étain* (tin oxide) (Fig. 4) in its catalogues. Moreover, it is known that Lefranc natural organic pigments were commonly modified with synthetic ones [22], therefore more analyses are needed to identify the content of the purple paint.

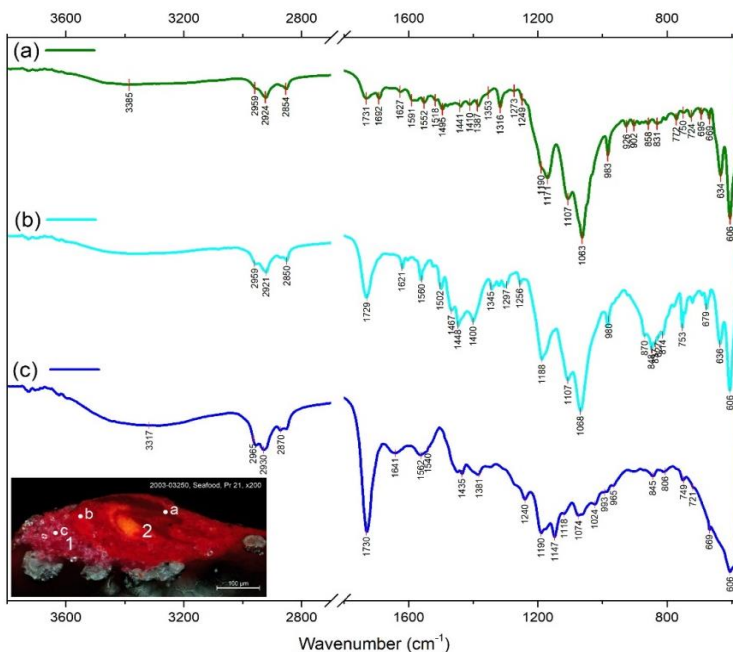


Fig. 7. μ FTIR spectra from sample 21: (a) layer 2 contains alizarin crimson and Hansa yellow, among other pigments; (b) layer 2 contains Hansa red, among other pigments; (c) layer 1 contains brazilwood, alizarin crimson and starch

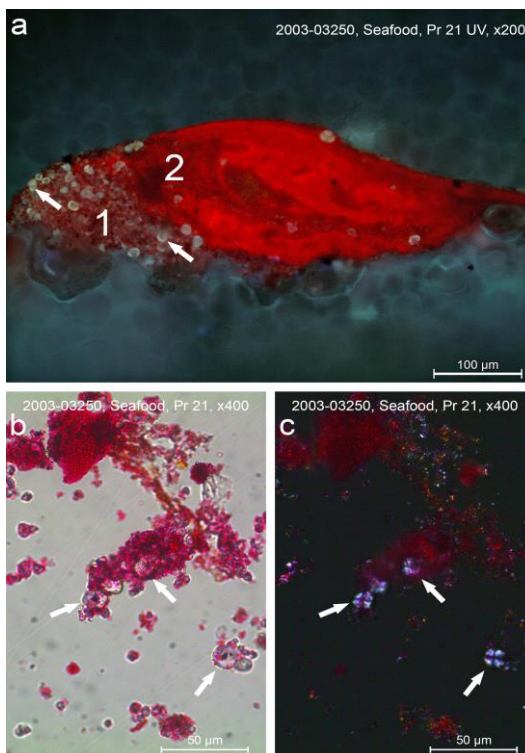


Fig. 8. Microscopy images showing (a) cross-section of sample 21, photographed in UV; (b) PLM pigment dispersion from layer 1 in plane light; (c) polarized light. Round, blue-fluorescing particles of starch are visible in (a) layer 1. Individual particles of starch were detected in (b) plane and (c) polarized light

The analysis of sample 21 revealed a very interesting aspect of Liu Kang's palette as he used two different types of red. One is composed of alizarin crimson, Hansa red and Hansa yellow with possible artist's admixture of chrome yellow; the second is a mixture of alizarin crimson and brazilwood on tin and starch substrate.

White

The UVR photography of the painting was very effective, given a preliminary indication that the plate was painted with lead white (Fig. 9).

Zinc white (zinc oxide) and titanium white (titanium dioxide), being strong absorbers, appear dark in UVR, and only the lead white among the white pigments reflects UV and appears white [5]. The SEM-EDS analysis of paint samples 22 and 10b, taken from the rim and bottom of the white plate, revealed a high concentration of Pb. The absorption bands in the FTIR spectra of sample 10b at 681, 853, 1040 and 1398 cm^{-1} are characteristic of lead white [30]. The SEM-EDS detection of Ba in sample 22 could be related to barium white, a common extender for lead white [31]. In both samples, the high content of Ca recorded with SEM-EDS, together with apparent absorption bands at 713, 872 and 1398 cm^{-1} in the FTIR spectra of sample 10b, indicates an admixture of chalk. It is worth noting that the 1398 cm^{-1} band, attributed to the antisymmetric stretching of CO_3^{2-} is assigned to the lead white as well as chalk. The presence of chalk is additionally confirmed by PLM observation (circular coccoliths). Other trace elements, like Si, Mg, Cr and Al, are considered as contaminants. Liu Kang used drying oil as a binder, and this is confirmed with FTIR in the sample 10b by peaks at 1173, 1730, 2852 and 2922 cm^{-1} [32].



Fig. 9. The UVR image of *Seafood* indicates that the plate was painted with lead white showing a strong UV reflectance

Black

Liu Kang used black paint extensively, with no hesitation, to enhance and isolate various forms from each other (Fig. 1). The elemental analysis of the sample taken from the shadow area beneath the table (sample 6b) recorded a high concentration of Ca and P, which can be attributed to bone black. A small concentration of Cr was attributed to viridian with PLM, while a concomitant presence of Cu and As suggested emerald green. Both green pigments can be considered as contamination from the artist's brush.

A summary of the identified materials from the *Seafood* is given in Table 1.

Table 1. Pigments detected in the painting *Seafood* by SEM-EDS, FTIR and PLM
 *Major elements are given in bold, minor elements in plain type and trace elements in brackets

Sample	Colour/ stratigraphy layer	SEM-EDS detected elements*	SEM-EDS assignment	possible	FTIR	PLM identification
4B	Light brown	C, O, Pb, Fe, Ca, Al, Si, Ba, Cr, (Sr, K, Mg, P)	Brown iron oxide, chrome yellow, chalk, bone black, barium white			Brown iron oxide, chrome yellow, chalk, bone black
13	Dark brown	C, O, Fe, Pb, Si, Ca, Cr, Al, (Ba, Zn, K, P, Na, Mg)	Brown iron oxide, chrome yellow, chalk, bone black, barium white			Brown iron oxide, chrome yellow, chalk, bone black
7	Light green	C, Pb, O, Ba, Cr, S, Al, As, Cu, (Ca, Fe, Si, P)	Viridian, chrome yellow, barium white, chalk, emerald green, brown iron oxide, Prussian blue		Chrome yellow, chalk, emerald green, Prussian blue, oil	Viridian, chrome yellow, brown iron oxide, Prussian blue
3	Dark green	O, C, Cr, Cu, Pb, Ba, As, Ca, Fe, S, (Si)	Viridian, emerald green, barium white, brown iron oxide, possible traces of Cr-containing yellow pigment(s)			Viridian, brown iron oxide,
21	Red	O, Ba, Pb, S, Sn, Ca, Cr, (Cl, Si, Na, Sr, Al, P)	Lead white, chrome yellow, chalk, barium white, tin substrate		Lead white, chrome yellow, chalk, barium white, alizarin crimson, Hansa red, Hansa yellow, oil	Chrome yellow, organic red, Hansa yellow
	Purple	C, O, Sn, Pb, (Ba, Ca, Si, Al, S, Cl)	Tin substrate		Brazilwood, alizarin crimson, starch, oil	Organic red, starch
10B	White	Pb, C, O, Ca, (Si, Mg, Cl, Na, Al)	Lead white, chalk		Lead white, chalk, oil	Lead white, chalk
22	White	Pb, C, O, Ca, (Si, Cl, Na, Ba, Mg, Cr, Al)	Lead white, barium white, chalk			Lead white, chalk
6B	Black	O, C, Ca, P, Pb, Zn, (Cu, Na, Si, Cr, Ba, As, K, Mg, Al, Sr)	Bone black, viridian, emerald green			Bone black, viridian

Hidden painting beneath Seafood

Pictorial composition

Racking light photography and digital microscopy of the paint surface of *Seafood*, revealed some anomalies. The most obvious are the brushstrokes of different colours that are visible through the very thinly applied brown paint of the table (Fig. 10a and b). This feature can be explained by the lack of an intermediate ground layer between the two compositions and, possibly, the decreasing hiding power of the upper paint layer [33, 34]. Severely cracked paint of the *Seafood* allowed to see different colours beneath (Fig. 10c and d). Moreover, some areas of the different paint scheme were not completely covered with the current painting (Fig. 10e and f). Additionally, by tracing the texture details in the racking light the existence of a portrait painting in a vertical orientation was revealed (Fig. 11a).

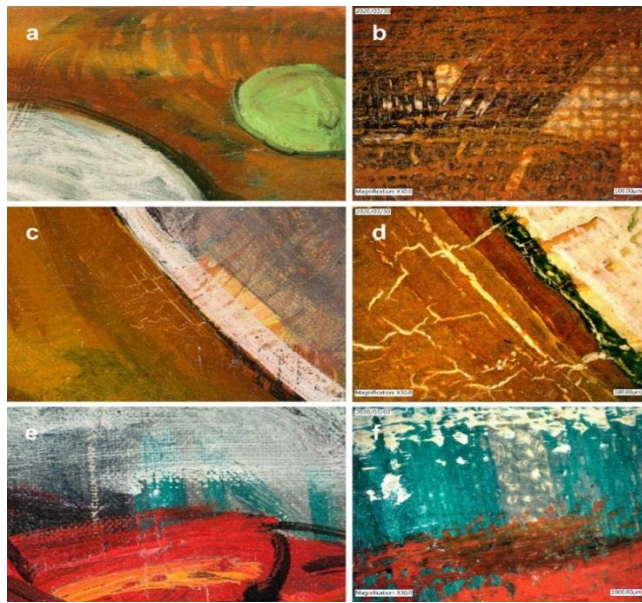


Fig. 10. Details showing: (a, b) individual brushstrokes of different colours visible through a very thin paint layer; (c, d) yellow paint of the earlier composition visible through cracks; (e, f) areas of earlier composition not completely covered with the current painting

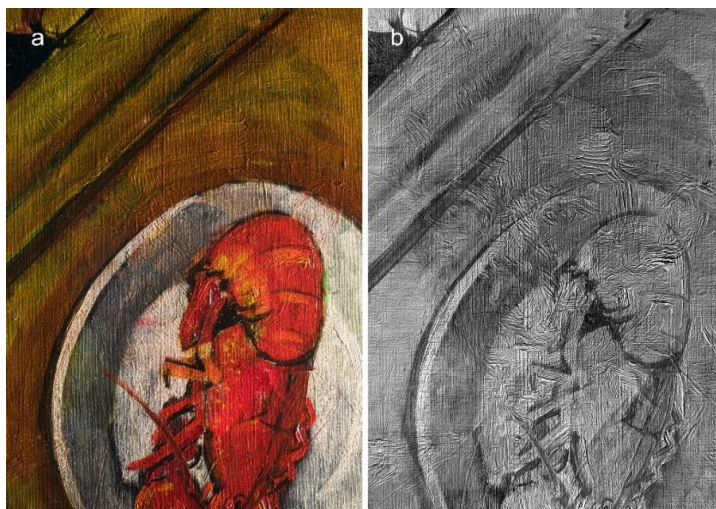


Fig. 11. Detail of the centre of *Seafood*, rotated at 90° clockwise and photographed in: (a) racking light and (b) NIR RTI. Racking light photography reveals the existence of a portrait painting in vertical orientation, while NIR RTI specular enhancement shows the surface texture with the reduced distraction of pictorial elements in *Seafood*

Subsequent NIR and transmitted NIR photography immediately unveiled a head-and-shoulders portrait view of a man wearing a collared shirt and suit jacket (Fig, 12a and b).

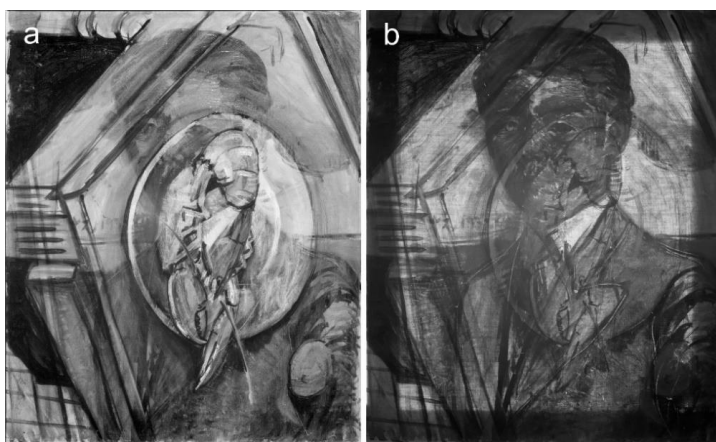


Fig. 12. Images of the painting *Seafood* rotated at 90° clockwise photographed in: (a) NIR and (b) transmitted NIR. Both photography techniques revealed a detailed portrait view of a man

His face is in the focal point and captured in $\frac{3}{4}$ view. The face details, along with the individual brushstrokes, are more legible in transmitted NIR, which provides good contrast and reduces interference from the upper composition. NIR sensitivity to carbon-based pigments, suggests that a dark paint containing carbon was used extensively for enhancing the shapes of the portrait painting. Carbon may also be present in the paint used for outlining in the upper composition, which obscures the visibility of the portrait underneath. Straight horizontal lines painted behind the subject's shoulders suggest an unknown background feature. In addition, the transmitted NIR showed the existence of thin white lines delineating the subject's suit jacket (Fig. 13).

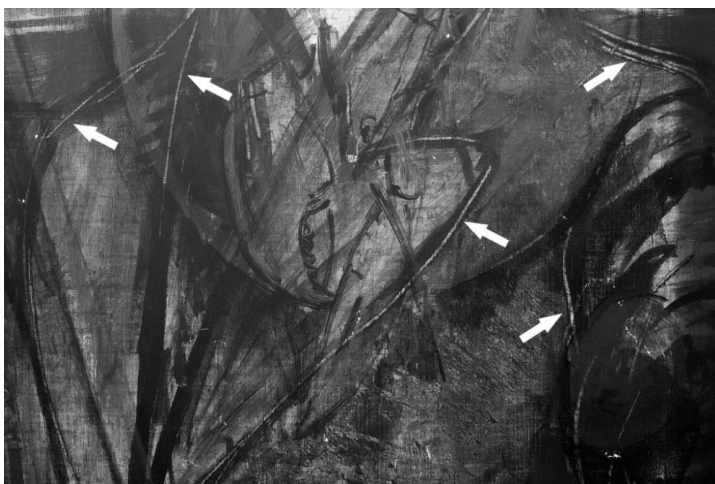


Fig. 13. Details of the portrait imaged by means of transmitted NIR photography, showing thin white lines delineating the subject's suit

The lines were probably achieved by scratching into wet paint with a sharp tool. This additional technique of artistic expression was found in another painting by Liu Kang, *Nude* from 1936 [35]. Transmitted NIR photography also unveiled Liu Kang's signature, in the horizontal orientation, painted in the corner between the subject's right shoulder and his head. It consisted of the Chinese character Kang (抗) followed by a partially legible date written in the Western style (1932) (Fig. 14).



Fig. 14. Detail of Liu Kang's signatures from the portrait beneath *Seafood*

The NIR-RTI photography technique was engaged to enhance the texture of the underlying portrait. Liu Kang applied short and multidirectional paint strokes with a small brush to define the shapes of eyes, nose, forehead and left ear, indicating an advanced paint build-up (Fig. 11b). Although a conventional RTI provides an improved view of the surface texture, replacing visible light with an infrared reduces the distraction from the pictorial elements in the upper paint layer due to the penetrative ability of the infrared [36]. Hence, the overall legibility of the paint texture of both *Seafood* and the underlying portrait was improved.

The acquired data was enriched by the XRR (Fig. 15), which appears as a positive image of the NIR.



Fig. 15. The XRR image of *Seafood* rotated at 90° emphasises the brushwork and reveals rather a sketchy handling of paint in the area of the face. The lack of the X-ray absorption in the centre of the forehead suggests very little or no paint in that area

The XRR additionally emphasised the brushwork and revealed a rather sketchy handling of the paint in the area of the face, which can be attributed to a young man with an oval face and a comb-over hairstyle. A strong X-ray absorption signal corresponds to the impastos recorded with the NIR-RTI. Intriguingly, there is a lack of X-ray absorption in the centre of forehead correlating with the transmitted NIR image, suggesting that this part of the painting was probably unfinished. In addition, below the horizontal background lines recorded with the NIR, the XRR revealed highly absorbent brushstrokes, which break the uniformity of space behind the subject.

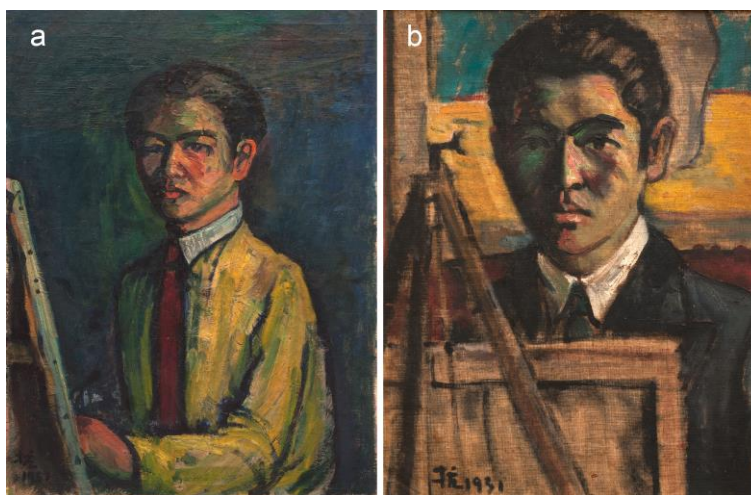


Fig. 16. Liu Kang's self-portraits: (a) *Self-portrait in Paris*, 1931, oil on canvas, 61 × 46cm; (b) *Self-portrait*, 1931, oil on canvas, 55 × 46cm. Liu Kang Family Collection. Images courtesy of Liu family

Knowing that the topic of self-portraits was explored by Liu Kang in Paris, a direct correlation of the hidden portrait was made with two self-portraits that were executed in 1931 and belonging to Liu family. The first, *Self-portrait in Paris*, is an oil-on-canvas painting, measuring 61 x 46cm. It features Liu Kang in a half-length self-portrait and $\frac{3}{4}$ face view (Fig. 16a). The second, *Self-portrait*, is also an oil-on-canvas painting measuring 55 x 46cm. It presents a head-and-shoulders portrait of Liu Kang captured in a full-face view (Fig. 16b).

The style of the revealed painting is entirely in accord with two other self-portraits. Both the revealed portrait and *Self-portrait* (Fig. 16b) are characterised by tight composition and a thin application of paint. Furthermore, the subject's $\frac{3}{4}$ face view and body position in the revealed portrait strongly resemble those in the *Self-portrait in Paris* (Fig. 16a). Based on the similarities in the style and composition in the three paintings, it is hypothesised that the portrait hidden beneath *Seafood* is another of Liu Kang's self-portraits.

Dating of self-portrait and reason behind its repainting

The stylistic similarity of the hidden painting with the two other self-portraits, as well as the partial legibility of its date, provides some evidence that the analysed painting was executed between 1930 and 1932. Based on the results from transmitted NIR and XRR photography (Figs. 12 and 15), it can be concluded that Liu Kang considered his work as completed as he signed and dated it. However, among his three self-portraits, this one (underneath *Seafood*) could have been unsuccessful, hence chosen by the artist for painting over with *Seafood* in 1932. The examination of the cross-sections of the paint layers revealed a clear stratigraphy and an absence of dirt between the layers corresponding to the *Seafood* and underlying self-portrait (Figs. 5a and 18d). These findings, combined with the distinct brushstrokes detected in the self-portrait (Figs. 11b and 15), strongly support the hypothesis that the time between the execution

of both the self-portrait and *Seafood* was relatively short, but sufficient for the paint on the self-portrait to dry before it was painted over. The practice of reusing earlier, unwanted paintings was – and still is – a common practice among artists, and it is known that two of Liu Kang's paintings from 1930 and 1936 were also executed on discarded compositions [35]. Archival photograph of Liu Kang in his rented room in Paris shows wall filled with unstretched paintings (Fig. 17). Based on this evidence, a conclusion can be drawn that Liu Kang's practice of reusing stretchers or strainers and unwanted paintings could have been measures to save on art materials so that he could continue with his painting studies.



Fig. 17. Liu Kang in his rented room in Paris in 1931 with wall tightly filled with paintings. Liu Kang Family Collection. Images courtesy of Liu family

Ground layer

SEM-EDS measurements combined with FTIR and PLM observations indicated that the composition of the ground layer (samples 10b, 19 and 22) is probably a mixture of lead white, barium white and chalk. Drying oil was used as a binder and exhibits typical peaks at 1173, 1731, 2851 and 2925 cm^{-1} [32].

Face

Concerning the paints and technique used for painting the face, the examination of the cross-sections, reveal that the flesh colour was achieved by the application of a yellow base tone, followed by darker paints. Yellow paint was found in the sample taken from the chin (sample 28), illustrated in Figure 18a and b. A similar yellow tone followed by brown, applied wet-in-wet, was observed in the cross-section of paint taken from the area between the nose and the right eye (sample 22), illustrated in the Figure 18c and d (layers 1, 2). However, a flesh tone on the cheek was achieved by a direct application of brown paint over the ground (sample 43), illustrated in Figure 18e and f.

Based on the SEM-EDS and PLM analysis, the yellow underpaint primarily involves a mixture of yellow iron oxide and lead white. A weak, SEM-EDS signal from P, Ca, Ba and Cr can suggest traces of bone black, barium white and/or barium yellow. Some contaminants, like Cr-containing green, were identified in sample 22 (layer 1). The brown and yellow layers have a similar elemental composition; however, the PLM allowed the observation of an admixture of organic red in the sample 43. The detection of red iron oxides corresponds to the yellow-green colour in the IRFC image of the examined areas (Fig. 3).

Vivid red lips (sample 10b) can be seen in visible light through a thinly applied white paint of the current composition (Fig. 1). Based on the SEM-EDS and FTIR analysis, the red paint probably contains a complex mixture of lead and barium whites, chalk and bone black. FTIR measurements detected anthraquinone derivative peaks at 939 and 1276cm^{-1} , indicating a possible use of alizarin crimson, while peaks at 752 and 1504cm^{-1} indicated a presence of Hansa yellow [37]. Liu Kang used drying oil as a binder; this is confirmed with FTIR by peaks at 1733 , 2852 and 2918cm^{-1} [32].

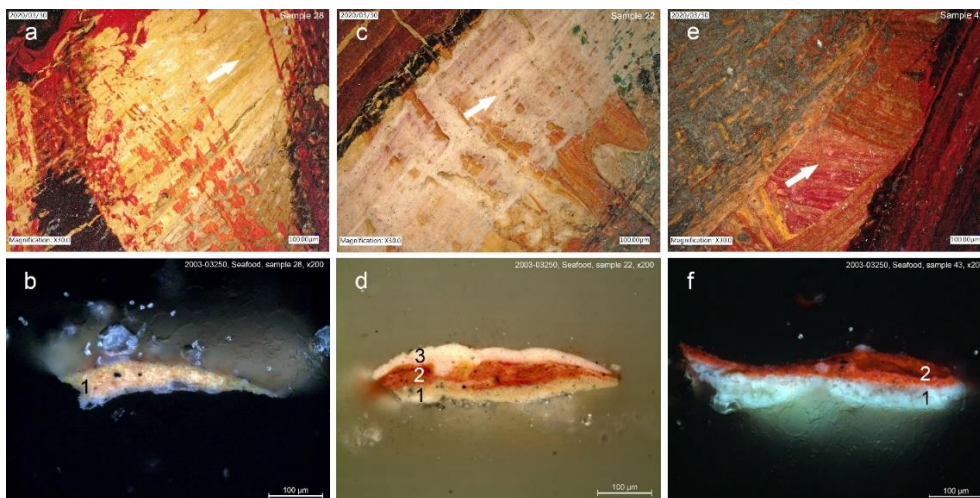


Fig. 18. Sampling sites and relevant cross-sections showing the structure of the paint layer in the area of the subject's face. The white arrows indicate the sampling sites. The microphotographs relate to: (a, b) sample 28 from chin; (c, d) sample 22 from the area between the nose and right eye; (e, f) sample 43 from cheek. Sample 22 contains a white top layer (layer 3) relating to the white plate in *Seafood*. This sample shows no evidence of an intermediate ground layer between the two painted compositions

Garment

The man's garment was assessed based on the fragments of the original composition that were not completely covered with the current painting.

The vivid, dark green colour found in the area of the suit's jacket lapels turns purple in the IRFC image (Fig. 19a and b) This observation is in agreement with the SEM-EDS and PLM identification of viridian probably in combination with lead white, bone black and barium white or barium yellow (sample 19).

The thick, black brushstrokes defining the folds of the suit's jacket contain mainly bone black and viridian, which were identified with SEM-EDS and PLM. Admixtures of lead and barium whites and/or lithopone (mixture of zinc sulphide and barium sulphate) and/or barium yellow are suspected in the black paint, based on the SEM-EDS analysis. The weak Sr-signal may be associated with the presence of strontium sulfate impurity in barium white [31, 38]. The identification of viridian could be in agreement with the warm hue of the black paint imaged in IRFC.

The bottom part of the suit's jacket appears darker, with a green-blue hue. The SEM-EDS and PLM of sample 20 confirmed the prominent use of viridian and bone black with some admixtures of ultramarine and brown iron oxide, which is consistent with the IRFC as green-blue turns purple. The paint mixture also contains Pb and Ba elements, and that could be assigned to lead and barium whites.

Background

In terms of the background colours of the self-portrait, exposed passages of green, blue and red colours were investigated.

Light green was found mainly in the top-right and top-left quarters in the background of the self-portrait (Fig. 1). The SEM-EDS and PLM analyses of the green paint (sample 40) revealed that it was predominantly made of viridian with an admixture of brown iron oxide and brightened with lead and barium whites. The result is consistent with the IRFC as green was imaged purple (Fig. 19c and d).

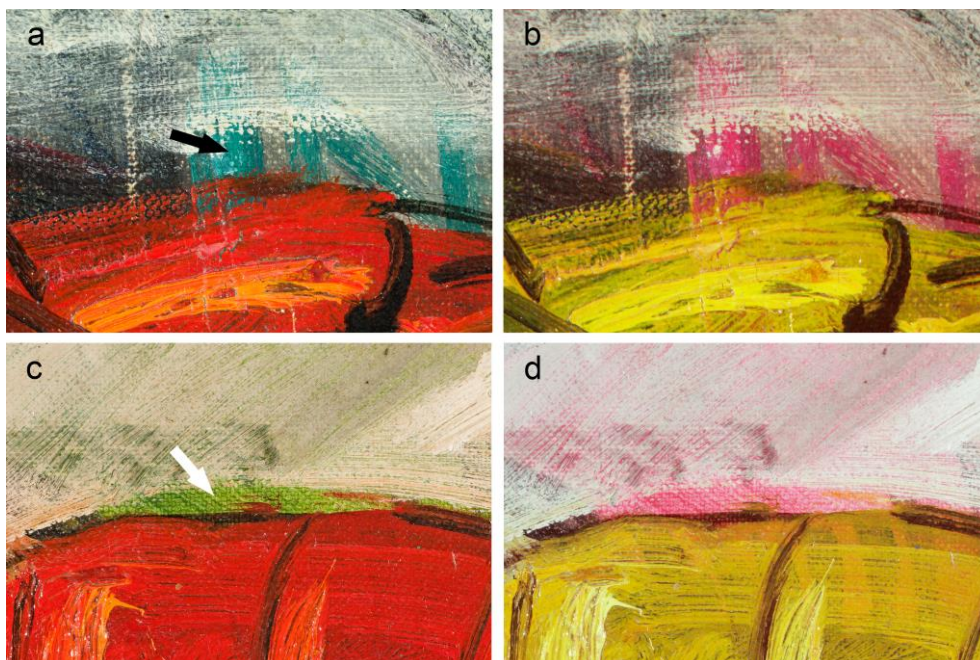


Fig. 19. Detail of *Seafood* photographed in visible light, showing green paint corresponding to the garment (a); background (c) of the self-portrait beneath; and (b, d) IRFC images of the same areas. The arrows indicate the extraction areas for sample 19 and 40

Grey-blue colour is largely visible in the bottom-left quarter of the background (Fig. 1). SEM-EDS combined with PLM of the grey paint (sample 11b) allowed for the identification of ultramarine and bone black with an admixture of viridian and brightened with lead and barium whites, which is agreeable with the grey-purple imaging of the area in IRFC (Fig. 3).

Red paint was recorded along the top edge of the self-portrait (Fig. 1), and it turned yellow in the IRFC (Fig. 3). In general, there was little distinction between the red and yellow pigments in the IRFC as they appeared as various shades of yellow. The XRF elemental analysis of spot 9 on the red paint detected the presence of Fe corresponding to the iron oxide, while Pb- and Cr-signals can be attributed to lead white and/or chrome yellow. Although a Ba-signal was not recorded, the trace of S could correspond to barium white; however, this assumption cannot be confirmed with only XRF analysis.

A summary of the identified materials from the self-portrait is given in Table 2.

Table 2. Pigments detected in the hidden self-portrait by SEM-EDS, FTIR, XRF and PLM.

Sample/spot	Colour/stratigraphy layer	SEM-EDS detected elements*	SEM-EDS, possible assignment	XRF	FTIR	PLM identification
22	Brown	C, O, Pb, Zn, Ba, Cr, Ca, Si, Fe, K, Al, (Na, S, Mg, P)	Iron oxide, lead white and/or chrome yellow, barium white and/or lithopone, Cr-containing yellow pigment(s)			
	Yellow	C, Pb, O, Ca, (Si, Fe, Al, Cr, Ba, Na, Mg)	Yellow iron oxide, lead white, barium white and/or barium yellow, Cr-containing green pigment			
	White (ground layer)	Pb, C, O, Ba, Ca, (Si, S, Na, Al)	Lead white, barium white, chalk			
28	Yellow	Pb, C, O, Ca, Si, Fe, (Al, Ba, Cr, Mg, P)	Yellow iron oxide, lead white, barium white and/or barium yellow, bone black			Yellow iron oxide, lead white
43	Brown	C, O, Ba, Pb, S, Si, Fe, Al, Cl, (Ca, P, K, Mg, Na)	Red iron oxide, lead white, barium white, bone black			Red iron oxide, organic red, lead white
10B	Red	Pb, C, O, Ca, Ba, Si, (Fe, Al, Sr, Mg, P)	Lead white, barium white, chalk, bone black, traces of iron oxide		Lead white, barium white, chalk, bone black, alizarin crimson, Hansa yellow, oil	
	White (ground layer)	Ba, C, O, S, Pb, Sr, (Ca, Si, Al)	Lead white, barium white, chalk		Lead white, barium white, chalk, oil	
19	Green	C, Pb, O, Cr, Ca, Ba, (Si, P, Na, Mg, Al, S)	Viridian, lead white, bone black, barium white or barium yellow			Viridian, lead white, bone black
	White (ground layer)	Pb, Ba, C, O, S, Sr, (Cr, Ca, Si, Zn, Mg, P, Al)	Lead white, barium white, chalk			
45	Black	O, Pb, Ca, C, P, Ba, Cr, Si, Zn, Al, Na, (S, Fe, K, Mg, Cl, Sr)	Bone black, viridian, lead white, barium white and/or lithopone and/or barium yellow			Bone black, viridian
20	Green-blue	C, O, Cr, Pb, Ca, Ba, P, (S, Si, Na, Al, Fe, Mg, Zn)	Viridian, bone black, ultramarine, brown iron oxide, lead white, barium whites			Viridian, bone black, ultramarine, brown iron oxide
40	Green	C, O, Pb, Ba, Cr, Ca, Si, S, Fe, (Al, Na, Zn)	Viridian, brown iron oxide lead white, barium white			Viridian, brown iron oxide, lead white
11B	Grey-blue	C, Pb, O, Ba, Ca, Si, Al, S, Na, (Cr, P, K)	Ultramarine, bone black, viridian, lead white, barium white			Ultramarine, bone black, viridian, lead white
9	Red	** XRF Detected elements: Pb, Fe, Cr, Ca, S	Iron oxide, lead white and/or chrome yellow, barium white			

*Major elements are given in bold, minor elements in plain type and trace elements in brackets.

Conclusions

The combination of complimentary non- and micro-invasive techniques provided important technical information about the painting *Seafood* and explained the nature of its intriguing paint features. Technical photography played an important role in the process of

understanding the artwork and the artist's way of handling the paint. Transmitted NIR, NIR-RTI and XRR significantly expanded the field of research and permitted the visualisation of Liu Kang's self-portrait hidden behind *Seafood*. The revealed self-portrait is probably a part of the artist's exploration of this topic as it complements two other self-portraits on canvas from 1931. Based on the acquired data, the hidden self-portrait was executed between 1930 and 1932. It can be deduced that Liu Kang considered it as a completed artwork by signing and dating it. However, among his three self-portraits, this one could have been the most unsuccessful and hence chosen for repainting with *Seafood* in 1932. This decision could have been primarily driven by materials shortage. As the archival photographs suggest, Liu Kang was saving on auxiliary supports, therefore the practice of reusing unwanted paintings could have been motivated by the financial constraints.

IRFC imaging assisted at the tentative identification of the pigments and sampling for the SEM-EDS, FTIR, PLM and XRF measurements. The binding medium for the ground layer and the paints for the self-portrait and *Seafood* is drying oil. The analysis of the paint samples gave an insight into the pigments used by Liu Kang in both paintings, contributing to a still-growing database of his painting materials. The majority of identified pigments are consistent across the two artworks and include viridian, alizarin crimson, iron oxides, chrome yellow, Hansa yellow, bone black, lead and barium whites. In both paintings, viridian appears to be the preferred green pigment. Lead white is a primary white and the main component of the ground layer. Admixtures of Prussian blue and emerald green were detected in the *Seafood* while ultramarine appears in the self-portrait only. The FTIR analysis of red paint revealed that Liu Kang used two different types of red in *Seafood*. One is composed of alizarin crimson, Hansa red and Hansa yellow with the artist's admixture of chrome yellow. The second is a mixture of alizarin crimson and brazilwood on tin and starch substrate. These very interesting findings require further analysis to precisely identify the components of the red paints, and it would involve comparisons with the reds from Liu Kang's other paintings from the same period. Some ambiguity still remains in the interpretation of the XRF data acquired from the red paint from the background of the self-portrait. Ultimately, the results obtained from the complementary analytical techniques employed in this study may aid art historians in the evaluation of Liu Kang's early career. Further research on the revealed self-portrait should focus on the investigation of the partially legible date and the technological and stylistic comparisons with two other self-portraits belonging to Liu family.

Abbreviations

UVF: ultraviolet fluorescence; UVR: reflected ultraviolet; NIR: near-infrared; IRFC: infrared false-colour; RTI: reflectance transformation imaging; XRR: X-ray radiography; XRF: X-ray fluorescence; SEM-EDS: scanning electron microscope with energy dispersive spectroscopy; FTIR: Fourier transform infrared spectroscopy; OM: optical microscopy; PLM: polarized light microscopy.

Acknowledgements

The authors would like to thank Professor Jarosław Rogóż PhD at Nicolaus Copernicus University and Hanna Szczepanowska PhD at West Virginia University for reviewing this paper; the National Gallery Singapore for allowing us to analyse the paintings; the Heritage Conservation Centre for supporting this study; Gretchen Liu for sharing Liu Kang's family painting collection and the artist's archival materials; Kenneth Yeo Chye Whatt (Principal Radiographer from the Division of Radiological Sciences at Singapore General Hospital); and

Dr Steven Wong Bak Siew (Head and Senior Consultant from the Department of Radiology at Sengkang General Hospital) for facilitating the X-ray radiography; and Roger Lee (Assistant Painting Conservator from Heritage Conservation Centre) for his assistance at RTI.

References

- [1] K.C. Kwok, **Journeys: Liu Kang and his art = Yi cheng: Liu Kang qi ren qi yi**, National Arts Council, Singapore, 2000, p. 49.
- [2] A. Cosentino, *Identification of pigments by multispectral imaging; a flowchart method*, **Heritage Science**, **2**(8), 2014, pp. 1–2, doi:10.1186/2050-7445-2-8.
- [3] A. Cosentino, *Practical notes on ultraviolet technical photography for art examination*, **Conservar Património**, **21**, 2015, pp. 53–62, doi: 10.14568/cp2015006.
- [4] A. Cosentino, *Infrared technical photography for art examination*, **e-Preservation Science**, **13**, 2016, pp. 1–6,
http://www.morana-rti.com/e-preservation-science/2016/ePS_2016_a1_Cosentino.pdf.
- [5] J. Warda, **The AIC Guide To Digital Photography And Conservation Documentation**, AIC, Washington, 2011, p. 160.
- [6] C. Schroer, J. Bogart, B. Mudge, M. Lum, **Guide To Highlight Image Capture**, Cultural Heritage Imaging, 2013,
http://culturalheritageimaging.org/What We Offer/Downloads/RTI Hlt Capture Guide v2_0.pdf. [Accessed 28 April 2019].
- [7] C. Schroer, J. Bogart, B. Mudge, M. Lum, **Guide To Highlight Image Processing**, Cultural Heritage Imaging, 2011,
http://culturalheritageimaging.org/What We Offer/Downloads/rtibuilder/RTI hlt Processing Guide v14_beta.pdf. [Accessed 28 April 2019].
- [8] C. Schroer, J. Bogart, B. Mudge, M. Lum, **Guide to RTIViewer**, Cultural Heritage Imaging, 2013,
http://culturalheritageimaging.org/What We Offer/Downloads/rtiviewer/RTIViewer Guide v1_1.pdf. [Accessed 28 April 2019].
- [9] P. Mactaggart, A. Mactaggart, **A Pigment Microscopist's Notebook**, 7th rev, Somerset, 1998.
- [10] N. Odegaard, S. Carroll, W.S. Zimmt, **Materials Characterization Tests For Objects Of Art And Archaeology**, Archetype publications, London, 2000, pp. 128–129.
- [11] V. Otero, C. Carlyle, M. Vilarigues, M.J. Melo, *Chrome yellow in nineteenth century art: historic reconstructions of an artists' pigment*, **RCS Advances**, **2**, 2012, pp. 1798–1805,
<http://dx.doi.org/10.1039/c1ra00614b>.
- [12] H. Kühn, M. Curran, *Chrome yellow and other chromate pigments*, **Artists' Pigments: A Handbook of Their History and Characteristics, Vol. 1** (Editor: R.L. Feller), National Gallery of Art, Washington, 1986, pp. 190, 196, 207.
- [13] L. Helwig, *Iron oxide pigments: natural and synthetic*, **Artists' Pigments: A Handbook of Their History and Characteristics, Vol. 4** (Editor: B.H. Berrie), National Gallery of Art, Washington, 2007, pp. 64, 65, 73, 88.
- [14] D.C. Stulik, A. Kaplan, *Application of a handheld XRF spectrometer in research and identification of photographs* (Editors: A.N. Shugar and J.L. Mass), **Handheld XRF for Art and Archaeology**, Leuven University Press, Leuven, 2013, p. 111.
- [15] C. McGlinchey, *Handheld XRF for the examination of paintings: proper use and limitations*, **Handheld XRF for Art and Archaeology** (Editors: A.N. Shugar, J.L. Mass), Leuven University Press, Leuven, 2013, p. 155.

- [16] N. Balcar, A. Vila, *Chemical composition of artistic paint: Lefranc reference samples from the first half of 20th century*, conference poster, **From Can to Canvas. Early Uses of House Paints by Picasso and His Contemporaries in the First Half of the 20th Century**, Marseille and Antibas, France, 25-27 May 2011.
- [17] L. Monico, G. Van der Snickt, K. Janssens, W. De Nolf, C. Miliani, J. Verbeeck, H. Tian, H. Tan, J. Dik, M. Radepon, M. Cotte, *Degradation Process of Lead Chromate in Paintings by Vincent van Gogh Studied by Means of Synchrotron X-ray Spectromicroscopy and Related Methods. 1. Artificially Aged Model Samples*, **Analytical Chemistry**, **83**(4), 2011, pp. 1214–1223, <https://doi.org/10.1021/ac102424h>.
- [18] R. Newman, *Chromium oxide and hydrated chromium oxide*, **Artists' Pigments: A Handbook of Their History and Characteristics, Vol. 3** (Editor: E. West FitzHugh), National Gallery of Art, Washington, 1997, p. 281.
- [19] D. Buti, F. Rosi, B.G. Brunetti, C. Miliani, *In-situ identification of copper-based green pigments on paintings and manuscripts by reflection FTIR*, **Analytical and Bioanalytical Chemistry**, **405**, 2013, pp. 2699–2711, <https://doi.org/10.1007/s00216-013-6707-6>.
- [20] R. Newman, *Some Applications of Infrared Spectroscopy in the Examination of Painting Materials*, **Journal of the American Institute for Conservation**, **19**, 1980, pp. 42–46, <https://doi.org/10.1179/019713679806028977>.
- [21] I. Fiedler, M.A. Bayeard. *Emerald green and Sheele's green*, **Artists' Pigments: A Handbook Of Their History And Characteristics, Vol. 3** (Editor: E. West FitzHugh), National Gallery of Art, 1997, p. 238.
- [22] L. Legan, K. Retko, P. Ropret, *Vibrational spectroscopic study on degradation of alizarin carmine*, **Microchemical Journal**, **127**, 2016, pp. 36–45, <https://doi.org/10.1016/j.microc.2016.02.002>.
- [23] I. Degano, P. Tognotti, D. Kunzelman, et al., *HPLC-DAD and HPLC-ESI-Q-ToF characterisation of early 20th century lake and organic pigments from Lefranc archives*, **Heritage Science**, **5**(7), 2017, <https://doi.org/10.1186/s40494-017-0120-y>.
- [24] L.F.C. de Oliveira, H.G.M. Edwards, E.S. Velozo, M. Nesbitt, *Vibrational spectroscopic study of brazilin and brazilein, the main constituents of brazilwood from Brazil*, **Vibrational Spectroscopy**, **28**(2), 2002, pp. 243–249, [https://doi.org/10.1016/S0924-2031\(01\)00138-2](https://doi.org/10.1016/S0924-2031(01)00138-2).
- [25] A. Bernardino-Nicanor, G. Acosta-García, N. Güemes-Vera, J.L. Montañez-Soto, M. de los Ángeles Vivar-Vera, L. González-Cruz, *Fourier transform infrared and Raman spectroscopic study of the effect of the thermal treatment and extraction methods on the characteristics of ayocote bean starches*, **Journal of Food Science and Technology**, **54**(4), 2017, pp. 933–943, <https://doi.org/10.1007/s13197-016-2370-1>.
- [26] H. Schweppe, J. Winter, *Madder and alizarin*, **Artists' Pigments: A Handbook of Their History and Characteristics, Vol. 3** (Editor: E. West FitzHugh), National Gallery of Art, Washington, 1997, pp. 112, 131.
- [27] J. Kirby, M. van Bommel, A. Verhecken, **Natural Colorants for Dyeing and Lake Pigments. Practical Recipes and Their Historical Sources**, Archetype Publications, London, 2014, pp. 33, 78, 101.
- [28] H. Schweppe, H. Roosen-Runge, *Carmine – cochineal carmine and kermes carmine*, **Artists' Pigments: A Handbook of Their History and Characteristics, Vol. 1** (Editor: R.L. Feller), National Gallery of Art, Washington, 1986, pp. 263, 272.
- [29] M. van Bommel, M. Geldolf, E. Hendriks, *An investigation of organic red pigments used in paintings by Vincent van Gogh (November 1885 to February 1888)*, **Artmatters. Netherlands Technical Studies in Art, Vol. 3** (Editor: E. Hermens), 2005, pp. 128, 129.

- [30] M.H. Brooker, S. Sunder, P. Taylor, V.J. Lopata, *Infrared and Raman spectra and X-ray diffraction studies of solid lead(II) carbonates*, **Canadian Journal of Chemistry** **61**, 3, 2011, pp. 494–502, <https://doi.org/10.1139/v83-087>.
- [31] R.L. Feller, *Barium sulfate – natural and synthetic*, **Artists' Pigments: A Handbook of Their History and Characteristics, Vol. 1** (Editor: R.L. Feller), National Gallery of Art, Washington, 1986, pp. 47, 58.
- [32] I.C.A. Sandu, C. Luca, I. Sandu, V. Vasilache, M. Hayashi, *Authentication of the ancient easel paintings through materials identification from the polychrome layers - II. Analysis by means of the FT-IR spectrophotometry*, **Revista de Chimie**, **59**(4), 2008, pp. 384-387.
- [33] T.B. Brill, **Light, Its Interaction with Art and Antiquities**, Plenum Press, New York, 1980, p. 89.
- [34] D. Thurrowgood, D. Paterson, M.D. de Jonge, R. Kirkham, S. Thurrowgood, D.L. Howard, et al., *A Hidden Portrait by Edgar Degas*, **Scientific Reports**, **6**, 2016, Article Number: 29594, <https://doi.org/10.1038/srep29594>.
- [35] D. Lizun, *A preliminary study of Liu Kang's palette and the discovery and interpretation of hidden paint layers*, **Heritage Science**, **8**(1), 2020, Article Number 21, <https://doi.org/10.1186/s40494-020-0363-x>.
- [36] E. Kotoula, G. Earl, *Integrated RTI approaches for the study of painted surface*, **CAA2014. 21st Century Archaeology. Concepts, Methods and Tools. Proceedings of the 42nd Annual Conference on Computer Applications and Quantitative Methods in Archaeology** (Editors: F. Giligny, F. Djindjian, L. Costa, P. Moscati and S. Robert), Archeopress Archeology, 2015, pp. 123–134.
- [37] R.M. Silverstein, G.C. Bassler, T.C. Morrill, **Spectrometric Identification of Organic Compounds**, Wiley, New York, 1991, <https://doi.org/10.1002/oms.1210260923>.
- [38] D.C. Stulik, A. Kaplan, *Application of a handheld XRF spectrometer in research and identification of photographs*, **Handheld XRF for Art and Archaeology**, (Editors: A.N. Shugar and J.L. Mass), Leuven University Press, Leuven, 2012, p. 111.

Received: May 18, 2020

Accepted: February 12, 2021